Hysteresis and bistability in periodically paced cardiac tissue

Xiaodong Huang,[1] Yu Qian,[2] Xiaoming Zhang,[3,*] and Gang Hu[1,†]
[1]*Department of Physics, Beijing Normal University, Beijing 100875, China*
[2]*Nonlinear Research Institute, Baoji University of Arts and Sciences, Baoji 721007, China*
[3]*College of Physics Science and Technology, Shenzhen University, Shenzhen 518060, China*
(Received 8 December 2009; revised manuscript received 8 March 2010; published 4 May 2010)

Hysteresis in periodically paced cardiac tissue is an important issue due to its relevance to cardiac arrhythmias. In the present paper, the mechanism of hysteresis formation and the related properties are interpreted by numerically investigating the phase I Luo-Rudy model. A formula calculating the width of hysteresis is proposed and well confirmed by numerical simulations. We also find that hysteresis in cardiac tissue shows several characteristics due to couplings among cardiac cells which are absent in a single cell. The influences of the physiological parameters are studied in detail. The model dependence of hysteresis is elucidated by considering a number of well-known models of excitable media. Moreover, the influence of bistability on controlling arrhythmias is revealed.

DOI: 10.1103/PhysRevE.81.051903 PACS number(s): 87.19.Hh, 05.45.−a

I. INTRODUCTION

Hysteresis refers to memory or lagging effect, which has been found in many physical, chemical and biological systems. Cardiac hysteresis was first reported by Mines [1], who found that frog ventricles can show two possible patterns, 1:1 and 2:1, in response to a wide range of stimulation frequencies. Hysteresis phenomena may occur in various cardiac systems [2–6], and in action potential duration (APD) restitution curves [7].

Hysteresis in periodically paced cardiac cell or tissue is the major topic in the research of cardiac hysteresis. Hall *et al.* [8] explored the prevalence of hysteresis in bullfrog cardiac muscle in experiment and found two kinds of hysteresis: the $1:1 \leftrightarrow 2:1$ hysteresis and the $2:2(\text{alternans}) \leftrightarrow 2:1$ hysteresis. Later, Yehia *et al.* [9] reported the detailed numerical and experimental investigations of the $1:1 \leftrightarrow 2:1$ hysteresis in a single cardiac cell. Walker *et al.* [5] observed hysteresis between two kinds of alternans in guinea pig hearts. These works indicated that hysteresis phenomena come from some intrinsic properties of the cardiac myocyte. In order to interpret the hysteresis phenomena, possible ionic mechanisms [5,10] and nonlinear mapping models [11,12] were proposed.

Given the above theoretical and experimental studies on cardiac hysteresis, there are still some problems that need further investigations. Theoretically, a general dynamical mechanism is still needed to interpret cardiac hysteresis. In the previous works hysteresis was discussed in a single cell [3,9,10] or tissue [5,6,8] separately, but the associations and differences of hysteresis between a single cell and tissue are rarely discussed. Furthermore, the influences of parameters on cardiac hysteresis were partly discussed by some previous works [3,6] but still lack an overall knowledge. Since many excitable models were utilized to explore cardiac problems [13–15], the model dependence of cardiac hysteresis is a problem worth considering. Moreover, it has been found that hysteresis can induce arrhythmia [16], which is known as a fatal disease in human beings. Much effort has been done in controlling arrhythmias [17–20]. However, the evaluation of the effects of hysteresis and bistability on cardiac arrhythmias treatment is insufficient.

In this work, we study cardiac hysteresis with phase I Luo-Rudy (LRd91) model [21] and obtain some results. First, the mechanism and the condition of hysteresis in a single periodically stimulated cardiac cell are demonstrated by analyzing the properties of APD rate-dependence and strength-interval (SI) dependence. In particular, we propose a formula to calculate the width of hysteresis window, which is a crucial characteristic quantity of hysteresis. The theoretical results are well confirmed by numerical simulations. Second, the results of a single cell are extended to one-dimensional (1D) tissue. Some phenomena that are absent in a single cell are found, such as bistability with two kinds of alternans and space dependent hysteresis patterns. Third, the influences of the parameters on hysteresis are investigated in 1D tissue, and the understanding of these influences is helpful in predicting hysteresis in realistic cardiac systems. Finally, the spiral waves control related to hysteresis in two-dimensional (2D) cardiac tissue is illustrated.

The paper is organized as follows. In Sec. II we introduce the model and methods. In Sec. III the mechanism of hysteresis in a single cardiac cell and the necessary condition for its formation are elucidated. In Sec. IV we discuss hysteresis in 1D tissue, and reveal several features being absent in a single cell. In Sec. V the influences of physiological parameters on hysteresis are discussed. In Sec. VI the model dependence and the relevance of hysteresis to controlling spiral waves are illustrated. The last section provides a summary of the results.

II. MODEL AND METHODS

The differential equation for the dynamics of the cell's membrane potential V_m (mV) is

*xmzhang@szu.edu.cn
†ganghu@bnu.edu.cn

$$C_m \frac{dV_m}{dt} = -I_{\text{ion}} + I_{\text{st}}(t), \tag{1}$$

where $C_m = 1\ \mu F/\text{cm}^2$ is the membrane capacitance, $I_{\text{ion}}(\mu A/\text{cm}^2)$ is the total transmembrane ionic current and $I_{\text{st}}(\mu A/\text{cm}^2)$ is the stimulating current. In LRd91 model, the total ionic current I_{ion} is the summary of six individual ionic currents

$$I_{\text{ion}} = I_{\text{Na}} + I_{\text{si}} + I_K + I_{K1} + I_{Kp} + I_b, \tag{2}$$

where $I_{\text{Na}} = G_{\text{Na}} m^3 hj(V_m - E_{\text{Na}})$, $I_{\text{si}} = G_{\text{si}} df(V_m - E_{\text{si}})$, $I_K = G_K XX_i(V_m - E_K)$, $I_{K1} = G_{K1} K1_\infty(V_m - E_{K1})$, $I_{Kp} = G_{Kp} Kp(V_m - E_{Kp})$, $I_b = G_b(V_m - E_b)$. Here m, h, j, d, f, and X are gating variables and the evolvement of each of them satisfies

$$\frac{dy}{dt} = \frac{y_\infty - y}{\tau_y}, \tag{3}$$

where y represents any gating variable, τ_y and y_∞ are the time constant and the steady state of y, respectively. The detailed description of this model was given by Luo and Rudy in Ref, [21]. Equation (1) is integrated by the explicit Euler method with time step $dt = 0.02$ ms. The gating variable equation is solved by the Rush-Larsen method [22]. All parameters are set to be the same as the original LRd91 model unless specified otherwise.

Bifurcation diagram of APD vs pacing cycle length (PCL) will be used to depict hysteresis and some other related phenomena such as alternans. When PCL is changed downward and upward in a loop, hysteresis can be formed in the bifurcation diagram.

III. HYSTERESIS IN A SINGLE CARDIAC CELL

It is known that the response of a cardiac cell to a long PCL is in 1:1 synchronization. However, as PCL is decreased, 1:1 synchronization may lose its stability and the response state can be substituted by Wenckebach period (WP) (i. e. N+1:N), alternans and 2:1 for low, high and intermediate magnitude of stimulating, respectively. In Fig. 1 we summarize the entrainment behaviors and find that hysteresis can emerge in the cases of direct 2:1 transition and period doubling bifurcation for intermediate stimulating magnitudes [Figs. 1(c) and 1(d)].

Hitherto two main approaches have been employed to interpret cardiac hysteresis: the ionic mechanisms [5,10] and nonlinear maps [8,9,12]. However, another approach can be proposed to interpret hysteresis qualitatively and quantitatively. In Refs. [11,12,23], the detailed description of the entrainment behaviors including hysteresis as shown in Fig. 1 was given by analyzing both ionic models and nonlinear maps. It was concluded that APD and excitability of a cardiac cell determine the bifurcation processes. Based on their researches, we go further to study hysteresis phenomena in a single cardiac cell by analyzing the properties of the dynamic APD restitution curve (DAPDRC) and the strength-interval curve (SIC).

APD restitution curve, representing APD as a function of diastole interval (DI), was first introduced by Nolasco and Dahlen [24] and further developed by Guevara *et al.* [25]. It is often used to predict the entrainment behaviors of cardiac systems under repetitive stimulations [12], such as 1:1 synchronization and alternans. In particular, DAPDRC is measured by the dynamic protocol: The system is paced at a constant PCL until steady state (regular N:M entrainment) is reached. After the DI-APD data pairs of the entrainment are recorded, PCL is changed and the process is repeated. Note that high enough amplitude of pacing should be used so that the slope >1 region of the DAPDRC (if such a region exists), which relates to alternans, can be displayed. In Fig. 2(a) only the entrainment responses of 1:1 and alternans (2:2) are plotted to construct the DAPDRC for relevant analysis. Under a certain PCL, the steady APD and DI is represented by the intersection point of the DAPDRC and the line representing $T_{\text{PCL}} = T_{\text{DI}} + T_{\text{APD}}$. Here T_{PCL}, T_{DI}, and T_{APD} stand for the time length of PCL, DI, and APD in mathematical expressions. Variation in PCL may cause movement of the intersection point and thus changes the steady value of APD. Therefore, DAPDRC represents APD rate-dependence (i.e., APD dependence on PCL). Moreover, there is another method called S1S2 pacing protocol for measuring APDRC. The S1S2-APDRC depends on the previous S1 pacing and is often used to evaluate the effect of a premature stimulus [26]. Under certain parameter and pacing conditions, S1S2-APDRC is no longer invariant due to memory effect [6,7]. Vinet [6] partly attributed hysteresis to such a factor. However, the DAPDRC is unique while the memory effect is implied by SIC in our approach.

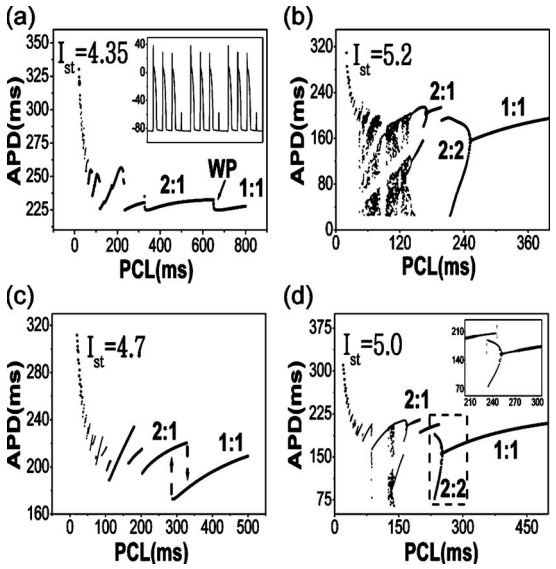

FIG. 1. Bifurcation diagrams of a single LRd91 cell at $G_{\text{si}} = 0.09$ and $G_K = 0.705$. Pulsatile stimuli with duration of 10 ms are used. The pulse magnitudes $[I_{\text{st}}(\mu A/\text{cm}^2)]$ are shown in figures. (a) Bifurcations of $1:1 \leftrightarrow \text{WP} \leftrightarrow 2:1$ without hysteresis for small I_{st}. 4:3 pattern in the WP region is shown in the small frame. (b) Bifurcations of $1:1 \leftrightarrow \text{alternans} \leftrightarrow 2:1$ without hysteresis for large I_{st}. (c) Bifurcations of $1:1 \leftrightarrow 2:1$ with hysteresis. (d) Bifurcations of $1:1 \leftrightarrow \text{alternans} \leftrightarrow 2:1$ with hysteresis.

The strength-interval curve depicts the minimum magnitude of the stimulus needed to induce an action potential (AP) as a function of the so called S1S2 interval [27]. It is

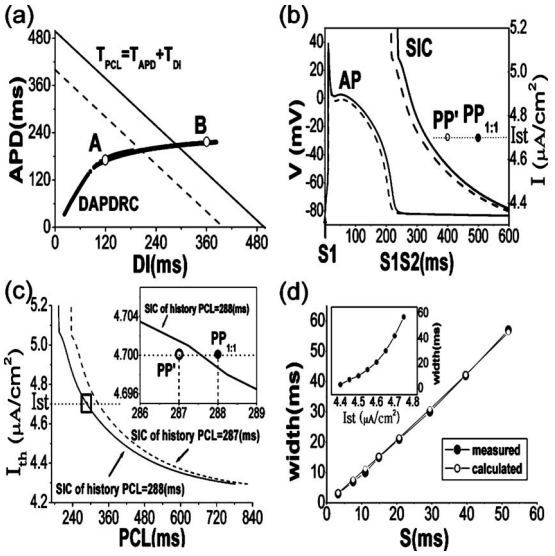

FIG. 2. Mechanism of hysteresis in a single cardiac cell. $G_{si}=0.09$ and $G_K=0.705$. (a) DAPDRC representing APD rate-dependence. The fact that the solid line moves to the dashed one corresponds to the process in (b). The transition that point A jumps to B corresponds to the process in (c). (b) Dynamics of PP, APD, and SIC responding to PCL changes. If PCL is decreased, $PP_{1:1}$ moves left to the empty circle PP′ and AP shrinks to the dashed one. Accordingly the solid SIC moves to the dashed one. (c) The process that SIC shifts rightward corresponding to the transition. The frame in the upper right area is the blowup of the small squared part. (d) The comparison of hysteresis width H measured from bifurcation diagrams (solid circles) and calculated by Eq. (4) (empty circles). The small frame depicts width H as a function of the stimulating magnitude.

created as follows: At first a stimulus (defined by S1) is delivered and an AP is successfully elicited. Then another stimulus (called S2) will be delivered at a wide range of time intervals relative to S1 (called S1S2 intervals). Each S1S2 interval requires a threshold magnitude (I_{th}) of S2 above which another AP can be elicited. Such a strength-interval relation constructs the SIC. Therefore, the location of SIC relies on the previous APD. Such dependence characterizes the "excitability memory of pacing history" [28]. Under periodical pacing situation, every stimulus can be viewed as S1, and S1 and S2 are identical. Then the time interval between any two successive stimuli (S1S2) is rightly the PCL. The cell's response to the change of PCL is determined by SIC.

For clarity, we analyze the $1:1 \leftrightarrow 2:1$ hysteresis, as shown in Fig. 1(c). The pacing with S1S2=PCL and magnitude $I=I_{st}$ can be regarded as a pacing point (PP) in the "S1S2-I" plane. The cardiac cell is initially paced by a long PCL and is in steady 1:1 state. The steady APD is represented by the intersection point of the DAPDRC and the solid line representing $T_{PCL}=T_{APD}+T_{DI}$ in Fig. 2(a). The PP and its resulting APD are shown in Fig. 2(b) by the solid circle labeled $PP_{1:1}$ and solid curve labeled AP, respectively. The SIC depending on the solid AP is shown by another solid curve labeled SIC. $PP_{1:1}$ is above SIC so that every stimulus is able to induce an AP during pacing. If PCL is decreased by ΔT_{PCL}, accordingly, the solid line in Fig. 2(a) moves downward by ΔT_{PCL}, and $PP_{1:1}$ in Fig. 2(b) moves left by ΔT_{PCL}. These movements lead to two cases:

Case 1: $PP_{1:1}$ moves left to the empty circle labeled PP′ [shown in Fig. 2(b)]. PP′ is still above the solid SIC so that 1:1 synchronization maintains. Meanwhile, the solid line representing $T_{PCL}=T_{APD}+T_{DI}$ shifts downward to the dashed one, as shown in Fig. 2(a), so that the steady APD is reduced by ΔT_{APD}. After steady state is reached, the SIC also moves left by ΔT_{APD} according to the reduced APD (this phenomenon is known as rate adaption). The steady AP and SIC at PP′ pacing is shown by dashed curves in Fig. 2(b). This dynamical process can be illustrated as: PCL decreases $\rightarrow$PP moves left$\rightarrow$APD reduces$\rightarrow$SIC shifts left. This process is repeated as PCL is decreased in 1:1 region. Since $\Delta T_{PCL}=\Delta T_{APD}+\Delta T_{DI}$ and $\Delta T_{PCL}>\Delta T_{APD}$, the moving distance of $PP_{1:1}$ at each PCL variation step is always larger than that of SIC so that $PP_{1:1}$ tends to approach SIC leftwards.

Case 2: there is a critical PCL. Once PCL becomes lower than this critical value, $PP_{1:1}$ moves slightly left to PP′ which locates below SIC [see the frame in the upper right area of Fig. 2(c)]. In this case the external pacing can no longer generate 1:1 response because its magnitude is smaller than the threshold, and 2:1 transition occurs. In Fig. 1(c), the transition from 1:1 to 2:1 occurs as PCL is decreased from $PCL_{1:1}=288$ ms to $PCL_{2:1c}=287$ ms. The steady APD under PCL=288 ms is represented by point A in Fig. 2(a) and the SIC corresponding to the steady APD is shown by the solid curve in Fig. 2(c). After the transition to 2:1 state, AP is induced by $2PCL_{2:1c}=574$ ms and the steady APD is represented by point B in Fig. 2(a). The transition that point A jumps to point B indicates enlargement of APD at the $1:1 \rightarrow 2:1$ transition. Due to such APD enlargement, the SIC jumps rightward to the dashed curve with an adaptive distance in Fig. 2(c). If PCL is increased now (PP′ is moved rightward in Fig. 2(c) and the dashed SIC moves rightward adaptively), we obtain 2:1 pattern in the original 1:1 region because PP′ is below the dashed SIC in this region. The PP′ has to move rightwards a much larger distance to chase up SIC and recover 1:1 state. The jumping backward of SIC determined by APD enlargement at the $1:1 \rightarrow 2:1$ transition point is the basic mechanism of hysteresis formation.

The above discussion indicates that APD enlargement is necessary for hysteresis. APD enlargement is associated to the slope of DAPDRC. If the slope is 0, APD is constant despite of PCL variations and no SIC shift will occur. Therefore, we obtain a necessary condition for hysteresis in a single cardiac cell: the slope of DAPDRC must be larger than 0. This condition guarantees the enlargement of APD and the jumping backward of SIC at the bifurcation point so that hysteresis may occur.

From the above analysis, we are able to derive an equation for calculating the width of hysteresis.

$$S = \int_{T_{PCL_{2:1c}}}^{T_{PCL_{2:1c}}+H} \frac{dT_{PCL}}{1+f'[T_{DI}(2T_{PCL})]}, \tag{4}$$

where S is the backward shift distance of SIC, H is the width of the hysteresis window and f' is the slope of DAPDRC at

the point that DI corresponds to the sTable II:1 solution. The integral begins from the critical point at which 2:1 transition occurs. The detailed derivation of Eq. (4) is given in the appendix. Figure 2(d) shows the comparison results of the hysteresis window width measured directly from bifurcation diagrams and computed by the analytical formula Eq. (4). The agreement is satisfactory. It should be noted that the stimulating magnitude may change the width [see the small frame in Fig. 2(d)] because, under different magnitudes, 2:1 transition may occur at different PCLs, and accordingly S and f' in the integral interval are different due to the nonlinearity of DAPDRC. The advantage of Eq. (4) is that H can be predicted without measuring point by point.

IV. HYSTERESIS IN ONE-DIMENSIONAL CARDIAC TISSUE

In this section we extend the investigation to cardiac tissue with diffusively coupled cardiac cells. For simplicity, we take 1D tissue as our example, then Eq. (1) should be modified to be

$$\frac{\partial V_m(x)}{\partial t} = \frac{-I_{\text{ion}} + I_{\text{st}}(x,t)}{C_m} + D\nabla^2 V(x). \tag{5}$$

We take $D=0.001$ cm^2/ms and the space step $dx=0.028$ cm for numerical simulations. In the simulations, no flux boundary condition is used, and $I_{\text{st}}(x,t)$ is applied at the left boundary of the tissue in the form of sinusoidal stimulation with amplitude 50 $\mu A/\text{cm}^2$. The sampling data are recorded from the cardiac cell 4.2 cm distant from the pacing site. The behaviors in 1D tissue are much more complicated than those in a single cell [29,30]. In the following, we classify several different kinds of hysteresis.

NHA: no hysteresis but alternans can be seen.

H2A: hysteresis between two alternans states.

HA: hysteresis window in which either branch (1:1 or 2:1 branch) bifurcates to alternans.

HIP: hysteresis widow including an irregular region. "Irregular" means that the response pattern looks chaotic and is essentially different from WP which should occur between 1:1 and 2:1 states in the single cell case.

HD: hysteresis caused by direct transition between 1:1 and 2:1.

NH: no hysteresis but transition between 1:1 and 2:1 can be seen.

The types of hysteresis NHA, HA, HD, and NH have already been revealed in a single cell (see Fig. 1). In real cardiac tissues, Hall *et al.* [8] found HA and HD and Walker *et al.* [5] found H2A in the experiments. In this section, we compare the hysteresis behaviors in a single cell and tissue, and give a brief explanation of how the differences come.

Comparing the hysteresis loops in a single cell with that in 1D tissue, we find that hysteresis in tissue occurs at lower PCL. Taking the parameter set of $G_{\text{si}}=0.055$ and $G_K=0.705$, for example, we alter the pacing waveforms and magnitudes to produce multiple hysteresis windows in both a single cell and 1D tissue. It is found that the left boundary of the window locates lowest at PCL=86 ms for a single cell while highest at PCL=73 ms for 1D tissue. This is because APD

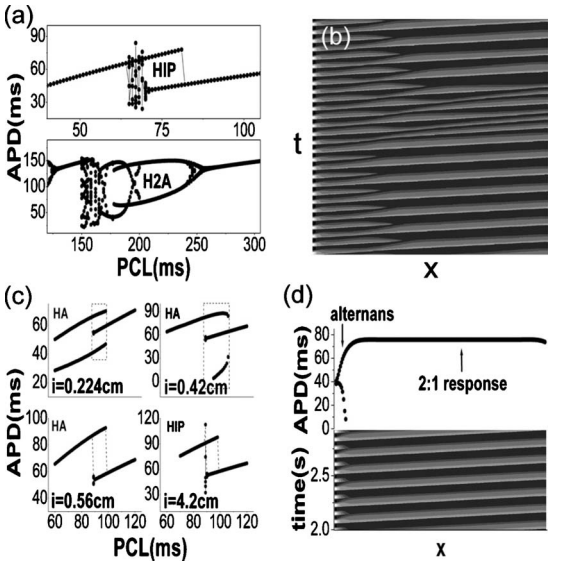

FIG. 3. Hysteresis in 1D cardiac tissue. $G_K=0.705$. (a) Bifurcation diagrams of HIP (upper frame, $G_{\text{si}}=0.055$) and H2A (lower frame, $G_{\text{si}}=0.07$). The data are measured at the point 4.2 cm distant from the pacing site. (b) Spatiotemporal pattern of the irregular region in HIP corresponding to the upper frame of Fig. 3(a). (c) $G_{\text{si}}=0.06$. Different types of hysteresis recorded at different sites for a same pacing loop. HA and HIP coexist in the tissue and even HA itself can show multiple forms. (d) $G_{\text{si}}=0.06$. Alternans and 2:1 response coexist in space under rapid pacing. Sites near the pacing boundary show alternans. Waves with smaller APD damp along the tissue (see the lower frame) and 2:1 response is identically realized for all cells far from the pacing.

in tissue is shortened by the diffusion term. Besides, some phenomena in 1D tissue which cannot occur in a single cell are found: (i) HIP shown in Fig. 3(a) (upper frame labeled "HIP") containing an irregular region where the system's responses look like chaotic and are different from WP. Figure 3(b) shows the spatiotemporal pattern of such a state. In fact the pattern is periodic. (ii) H2A shown in Fig. 3(a) (lower frame labeled "H2A") illustrating hysteresis between two kinds of alternans with different alternating amplitudes, which was revealed experimentally by Walker *et al.* [5] and now is found by numerical simulations. (iii) Interesting space dependent behaviors of hysteresis, i.e., the types of hysteresis at different space sites are different. Figure 3(c) illustrates this phenomenon by showing hysteresis patterns at different distances from the pacing site. In Fig. 3(d) we show that under rapid pacing we can observe alternans near the pacing site and 2:1 response far from the pacing site in the same tissue.

Conduction velocity (CV) dispersion relation representing the dependence of CV on DI is an important relation in tissue. In conduction along the tissue, the actual pacing interval of the ith cell $T_{\text{PCL}}(i)$ can be computed by

$$T_{\text{PCL}}(i) = T_{\text{PCL}} + \int_{x_{\text{st}}}^{x_i} \left\{ \frac{1}{v_{front}^{next}(T_{\text{DI}}(x))} - \frac{1}{v_{front}^{previous}[T_{\text{DI}}(x)]} \right\} dx \tag{6}$$

where $v_{front}[T_{\text{DI}}(x)]$ is the velocity of the wave front as a function of DI. In 1:1 state $v_{front}^{next}[T_{\text{DI}}(x)]=v_{front}^{previous}[T_{\text{DI}}(x)]$

and every cell has the same pacing interval $T_{\mathrm{PCL}}(i)=T_{\mathrm{PCL}}$. With the decrease in PCL and the resulted variations in APD and DI, velocities between successive wave fronts may be different and $T_{\mathrm{PCL}}(i)$ can thus be greater or smaller than PCL. Consequently, the APDs of cells along the tissue can also be different due to rate dependence. If PP of a certain cell is below its SIC, block occurs at this site. The above discussion indicates that propagation block in cardiac tissue is associated to three factors: dispersion of velocity, APD restitution property and coupling magnitude between cells. Wave propagation in cardiac tissue were investigated in detail by Courtemanche *et al.* [31] and Comtois *et al.* [32]. Because of block, there is sufficient recovery time for some coming waves to pass, and APDs of these waves vary significantly. That is why we can observe HIP behavior. Therefore, HIP can be seen only in tissue due to spatiotemporal complexity. For the similar reason, H2A and space dependent patterns can never been observed in a single cardiac cell. Nevertheless, the precise mechanisms of H2A in excitable cardiac tissue need further investigations.

V. INFLUENCES OF CARDIAC PARAMETERS

Since hysteresis influences the functions of realistic cardiac systems, it is thus important to identify the parameter conditions of hysteresis for some practical heart systems. Vinet [6] explored the influence of the potassium current theoretically. However, many ionic currents participate in forming an AP. It is significant to characterize the effect of each of the ionic currents on hysteresis.

In this section, we specify the parameter regions of cardiac hysteresis in LRd91 model by analyzing the effects of physiological parameters. This approach may be useful for providing drug therapy [33] and giving some suggestive ideas for hysteresis control. The simulations are performed in 1D tissue, and the data are recorded from the point 4.2 cm distant from the pacing site. Through these discussions, we may obtain an overall knowledge about how various realistic physiological quantities can affect hysteresis phenomena.

In a cardiac system, parameters alternating the ionic currents may also change the AP shape and accordingly influence the hysteresis behaviors. There are six ionic conductance parameters that govern the six fully activated ionic currents in the LRd91 model. The six conductance parameters are: G_{si}, G_b, G_K, G_{K1}, G_{Na}, and G_{Kp}, and the corresponding six currents I_{si}, I_b, I_K, I_{K1}, I_{Na}, and I_{Kp} can affect certain AP phases effectively [34]. The effects of the parameters on hysteresis are shown in Figs. 4 and Fig. 5. In Figs. 4 and 5, the six conductance parameters are changed in the intervals practical for realistic guinea pig hearts. These parameters can influence the type and the width of hysteresis by altering the DAPDRC slope. The results obtained in Figs. 4 and 5 can be summarized as: (i) the influences of the conductance parameters on hysteresis can be ranked as $G_{\mathrm{si}} > G_b > G_K > G_{K1} > G_{\mathrm{Na}} > G_{Kp}$. Among them, G_{si}, and G_{Kp} are the strongest and weakest parameters, respectively; (ii) There is a common sequence for the appearance of various types of hysteresis, which is actually determined by the DAPDRC slope: NHA→H2A→HA→HIP→HD→NH.

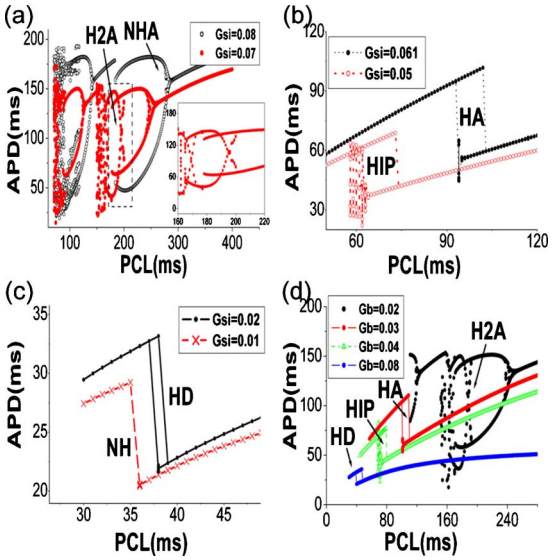

FIG. 4. (Color online). Influences of G_{si} (0.01–0.08) and G_b (0.01–0.08) on hysteresis. G_K=0.705 The parameter ranges are practical for realistic guinea pig hearts. (a) G_b=0.03921. NHA and H2A are observed for G_{si}=0.08 and G_{si}=0.07, respectively. (b) and (c) G_b=0.03921. HA→HIP→HD→NH occur in sequence in the G_{si} range between 0.06 to 0.01 and the hysteresis windows shift leftward as G_{si} decreases. (d) G_{si}=0.055. Influence of parameter G_b. The hysteresis behaviors are similar to that of G_{si} variations with NH being absent here. The absence of NH in (d) indicates that hysteresis cannot be eliminated by adjusting G_b only.

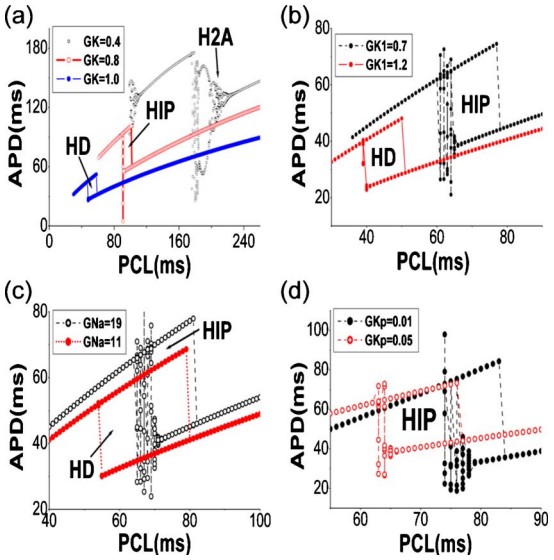

FIG. 5. (Color online). Influences of G_K, G_{K1}, G_{Na} and G_{Kp} on hysteresis. G_{si}=0.055 and G_b=0.03921. (a) and (b) G_K and G_{K1} are varied between 1.2 and 0.2. The windows are pushed leftward by the increase in the parameters. H2A is seen at G_K=0.4. (c) G_{Na} has much weaker influence on hysteresis in comparison with G_{si}, G_b, G_K and G_{K1}. Nevertheless, HIP can be eliminated by decreasing G_{Na}. Hysteresis window is shifted to the left much more gently by decreasing G_{Na} than that in (a) and (b). (d) The type of hysteresis remains invariant when G_{Kp} is varied in a wide range.

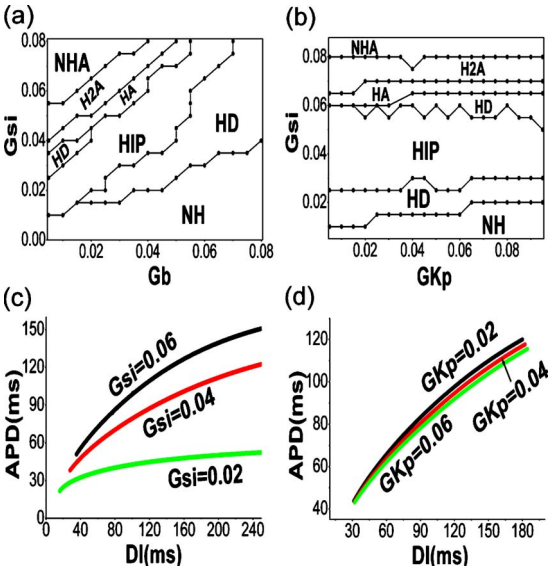

FIG. 6. (Color online). Parameter domains of various types of hysteresis in G_{si}-G_b plane (a) and G_{si}-G_{Kp} plane (b). G_K=0.705. From these figures the appearance sequence of various types of hysteresis can be seen. (c) and (d) show the effects of G_{si} and G_{Kp} on the DAPDRC slope. G_{si} has a much stronger effect than G_{Kp} so that G_{si} alters hysteresis behaviors much more intensely than G_{Kp}.

This sequence is shown clearly in Figs. 4(a)–4(c) when the slope decreases as G_{si} reduces; (iii) H2A could be obtained only by adjusting G_{si}, G_b, and G_K [see Fig. 4(a) for G_{si} =0.07, Fig. 4(d) or G_b=0.02 and Fig. 5(a) for G_K=0.4]. Walker [5] concluded that H2A is closely associated with the intracellular calcium cycling. The results in our numerical simulations suggest that hysteresis of alternans may also be influenced by potassium currents; (iv) variations reducing the DAPDRC slope push the left boundary of the corresponding hysteresis window leftwards. The left boundary of the window is determined by the smallest APD in 1:1 entrainment, so any variations shortening APD facilitate 1:1 maintenance and push the hysteresis window leftwards.

In Figs. 6(a) and 6(b), we show the parameter domains of hysteresis in G_{si}-G_b (the two physiological quantities influencing the hysteresis behaviors mostly) and G_{si}-G_{Kp} (one mostly and one least) planes, respectively. Although multiple types of hysteresis coexist in the tissue, beyond a certain distance from the pacing site (no more than 1 cm), cells in the tissue show the same type of hysteresis for a fixed set of parameters. We take this asymptotic behavior as the result. These diagrams give the instructive information about where one can find certain types of hysteresis and how one can control hysteresis phenomena by alternating parameters. The appearance order of various types of hysteresis is clearly shown in Figs. 6(a) and 6(b). Moreover, Fig. 6(b) verifies the previous conclusion that parameter G_{Kp} has very weak influence on hysteresis. Most importantly, we find that G_{si} is the only parameter for eliminating hysteresis [shown by the bottom lines in Figs. 6(a) and 6(b)]. At sufficiently low G_{si} the DAPDRC becomes flat and the SIC jumping is small so that the spatial diffusion can easily erase hysteresis. However, in the NH region of the tissue, we can still observe hysteresis in a single cell. According to this observation we expect that bistability in a cell is a necessary but not sufficient condition for bistability in tissue. The effects of G_{si} and G_{Kp} on DAPDRC slope are shown in Figs. 6(c) and 6(d). Figure 6 verifies the restitution of APD is the main contributor to hysteresis by revealing that: the more effectively the parameter acts on the repolarization and duration of action potential, the more greatly it influences hysteresis.

Pacing parameters, such as pacing waveform and amplitude, can also influence hysteresis in cardiac tissue [3]. We have used square and sinusoidal waveforms with different amplitudes and find that these factors can only change the width of hysteresis window or shift the parameter domain of hysteresis. The characteristics of cardiac hysteresis are not essentially changed by the pacing parameters.

VI. MODEL DEPENDENCE OF HYSTERESIS AND THE RELEVANCE OF BISTABILITY IN PACED CARDIAC SYSTEM TO SPIRAL WAVE CONTROL

In the above sections, hysteresis behaviors of LRd91 model are investigated in detail. There are many models of excitable media describing cardiac or chemical reaction dynamics. It is thus interesting to study whether the hysteresis behaviors are popular in the excitable media.

We have studied a number of excitable media and find surprisingly that the models mainly used for describing cardiac dynamics, such as Beeler-Rueter model (BR77) [35] and canine ventricle model (CVM) [36], exhibit clearly hysteresis features like LRd91 model, while other models, which describe general excitable media, such as Bär [37] and FHN models [39], can never show hysteresis. The mechanism underlying the model dependence of hysteresis is heuristically explained in Fig. 7. According to the analysis in Sec. III, a necessary condition for hysteresis is that the DAPDRC of the given system must have slope larger than 0, so that APD can enlarge when 2:1 occurs and hysteresis can take place. Figure 7 shows DAPDRCs of various excitable models. Figures 7(a)–7(d) exhibit DAPDRCs of cardiac models with slope greater than 0 [see Figs. 7(a) and 7(c)] and the corresponding hysteresis [see Figs. 7(b) and 7(d)]. In Figs. 7(e) and 7(f), DAPDRCs of the general excitable models are in a flat shape with slope being approximately 0. This is the reason why hysteresis occurs in certain cardiac models but not in some general excitable models.

Physically, arrhythmias control is to suppress spiral and turbulent waves (corresponding to ventricular tachycardia and ventricular fibrillation in mammal heart [40]) in cardiac tissue [17,18]. Although hysteresis may violate the ordered heart rhythm [16], it can also help to recover the normal heart rate. In the previous works of controlling arrhythmias [19,20] such a factor was rarely noticed. In the following, we will show how hysteresis and bistability "help" arrhythmias control in LRd91 model.

We use the boundary overdrive pacing (BOP) method which has been widely used in experiments and theoretical works [19,20] as a low damage control method. The proper pacing frequency is often chosen before the action from the

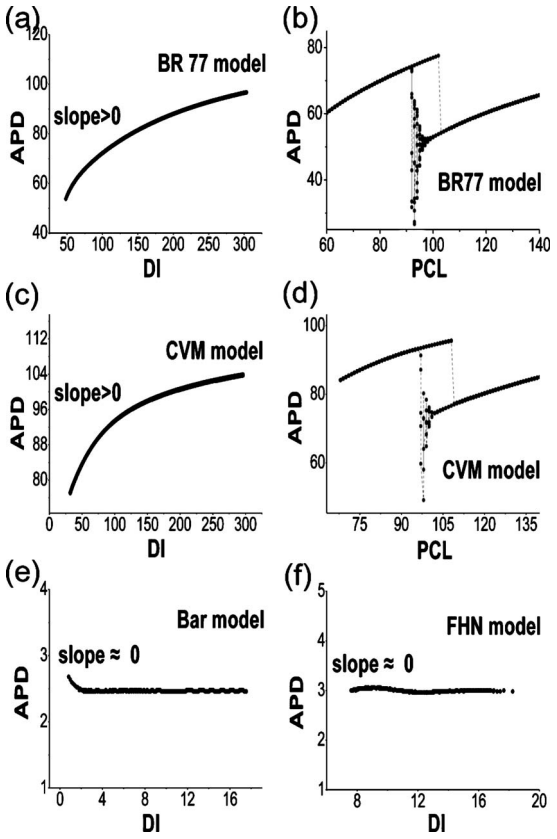

FIG. 7. Model dependence of hysteresis behavior. Parameters of the models are set to be the same as their original forms except: G_s=0.05 (BR77 [35]); $PCa\_$=1.26×10^{-5} (CVM [36]); a=0.84, b=0.07 and ε=0.06 (Bär [37]); β=0.7, γ=0.5, and ϵ=0.302 (FHN [38,39]). All the simulations are performed in 1D tissue. (a) and (b) DAPDRC of BR77 model and the corresponding hysteresis. (c) and (d) DAPDRC of CVM model and the corresponding hysteresis. (e) and (f) DAPDRCs of Bär and FHN models with slope approximately equals to 0.

"drive-response" relation because the successful BOP control must satisfy the condition that the controlling waves induced by the pacing signals must have frequencies higher than those of spiral or turbulent waves [20,41]. This is because of the rule that fast waves win the competition against slow waves in all excitable media. From Fig. 8(a), it seems that the spiral or turbulent waves with frequency f_s can never be controlled, because the frequency is higher than the maximum frequency $f_{\max}$ produced by the BOP method in the given LRd91 tissue. However, to our surprise, we did succeed to suppress spiral waves of $f_s > f_{\max}$. The key mechanism underlying this phenomenon is the bistability behavior in the cardiac tissue.

Though the drive-response curve of Fig. 8(a) shows the maximum frequency $f_{\max}$ lower than that of the spiral waves (the target to be controlled), there is another branch of hysteresis shown in Fig. 8(b) by empty circles where the frequencies of the controlling waves 1:1 synchronize to the pacing. Thus the frequency of the controlling waves (CWs) can be higher than that of the spiral waves (SWs), and the higher frequency can be realized under the initial condition of SWs (not under the initial rest state). These pacing-generated waves can successfully suppress the SWs.

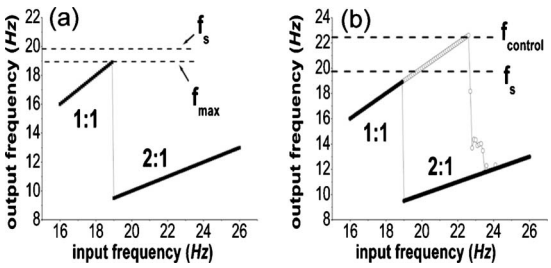

FIG. 8. Drive-response curves in LRd91 model. G_{si}=0.035, G_K=0.705 and the other parameters are the same as Ref [21]. The frequency of spiral waves is f_s=19.7 Hz. (a) Drive-response relation of the tissue measured from the homogeneous rest state. The spiral waves frequency f_s is slightly higher than $f_{\max}$. (b) Bistability obtained from initial condition of spiral waves. Empty circles enlarge the 1:1 region where the response frequencies can be higher than $f_{\max}$ and f_s.

Figure 9 shows our experiment in 2D tissue. First, we use BOP with frequency f_c=22.4 Hz on the left boundary to produce a train of CWs in the rest cardiac tissue. The CWs propagate with frequency f_{cp}=0.5f_c for 2:1 entrainment. At t=1.5 s a plane wave front is cut and SWs develop after then. This process simulates the situation that CWs encounter SWs during propagation. The frequency of the SWs is f_s=19.7 Hz>f_{cp}=0.5f_c (f_c=22.4 Hz) so that SWs defeat the CWs and occupy the whole tissue eventually. However, after the SWs invade the pacing region, the CWs are perturbed and flip to 1:1 branch, and then the CWs obtain the frequency f_c higher than that of SWs ($f_c > f_s$). From t=4 s, CWs start to eliminate the SWs. At t=14 s the CWs defeat SWs completely and the control is realized. The process in Fig. 9 virtually shows that CWs lose first and win at last due to the bistability of the response behavior.

VII. SUMMARY

In summary, we studied the problem of hysteresis in cardiac systems. By numerical simulations and theoretical analysis the following major results were achieved.

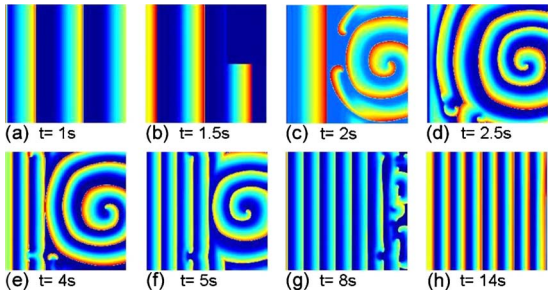

FIG. 9. (Color online). The process of how bistability help control. The tissue size is 420×420. G_{si}=0.035, G_K=0.705. The BOP is in sinusoidal waveform with frequency f_c=22.4 Hz and amplitude 50 $\mu A/cm^2$. (a) CWs propagate with a frequency f_{cp}=11.2 Hz for 2:1 response. (b) At t=1.5 s a plane wave front is cut. (c) SWs develop after then with a frequency f_s=19.7 Hz. (d) At t=2.5 s SWs fully develop and defeat CWs because $f_s > f_{cp}$. (e) As the CWs flip to 1:1 branch and obtain a higher frequency $f_c > f_s$, CWs gradually invade the tissue again. (f)–(h) CWs compete with SWs and CWs control the whole tissue at last.

First, by analyzing DAPDRC and SIC properties in the single cardiac cell system, we revealed the necessary condition for hysteresis: the slope of DAPDRC must be larger than 0. Based on this condition we obtained a formula to analytically calculate the width of hysteresis. The theoretical results are satisfactorily confirmed by the numerical results.

Second, we further studied 1D cardiac tissue and observed some phenomena including HIP, H2A and space dependent hysteresis, which cannot be found in a single cardiac cell. The reason is that the spatiotemporal complexity plays key roles in generating all these characteristics of hysteresis.

Third, we investigated how different physiological parameters influence hysteresis behaviors. We ranked the influences of various physiological parameters in such an order: $G_{si} > G_b > G_K > G_{K1} > G_{Na} > G_{Kp}$. Moreover, we also roughly ordered the sequence of the appearance of various types of hysteresis as NHA $\rightarrow$ H2A $\rightarrow$ HA $\rightarrow$ HIP $\rightarrow$ HD $\rightarrow$ NH, corresponding to the DAPDRC slope reduction. These understandings are significant for dealing with the hysteresis problems in practical cardiac systems.

Finally, we found that hysteresis phenomenon is strongly model dependent in excitable media. It is common in excitable models describing cardiac dynamics but it cannot be observed in some simplified while very popular excitable models. The dynamical mechanism underlying this model dependence is heuristically explained by the slope of the DAPDRCs of different models.

The problem how to treat arrhythmias is a challenging problem. Results in the present work show that the hysteresis behavior may have effect on promoting spiral waves control.

ACKNOWLEDGMENTS

This work was supported by the National Natural Science Foundation of China under Grants No. 10675020 and No. 10975015 and by the National Basic Research Program of China (973 Program) under Grant No. 2007CB814800.

APPENDIX: DERIVATION OF EQ. (4)

To obtain Eq. (4) is essentially to solve a traditional chasing problem. The "time" for PP chasing up SIC at distance S is the width of the hysteresis. It depends on the "velocity" difference between PP and SIC. The fact that PCL increases by ΔT_{PCL} is equivalent to the fact that PP shifts a distance of ΔT_{PCL} so that the velocity of PP is

$$v_{PP} = \frac{\Delta T_{PCL}}{\Delta T_{PCL}} = 1.$$

Because of the rate-dependence, ΔT_{PCL} prolongs APD and makes SIC walk a corresponding distance on the same direction. If we take the walking distance of SIC to be approximately the prolongation of APD, the velocity of the SIC is

$$v_{SIC} = \frac{T_{APD}(2T_{PCL} + 2\Delta T_{PCL}) - T_{APD}(2T_{PCL})}{2\Delta T_{PCL}},$$

where factor 2 is because of 2:1 state. The relation among the time lengths of PCL, APD, and DI is

$$2T_{PCL} = T_{APD}(2T_{PCL}) + T_{DI}(2T_{PCL})$$

so that

$$2\Delta T_{PCL} = T_{APD}(2T_{PCL} + 2\Delta T_{PCL}) - T_{APD}(2T_{PCL}) + T_{DI}(2T_{PCL} + 2\Delta T_{PCL}) - T_{DI}(2T_{PCL}).$$

Dividing the equation by $T_{APD}(2T_{PCL}+2\Delta T_{PCL}) - T_{APD}(2T_{PCL})$, and assuming ΔT_{PCL} to be sufficiently small, we can obtain

$$\frac{1}{v_{SIC}} = 1 + \frac{1}{f'(T_{DI}(2T_{PCL}))}$$

with f' being the slope of DAPDRC at the point that DI corresponds to the sTable II:1 solution. We can see that v_{SIC} is always smaller than 1 so that PP can chase up SIC at sometime.

The time H for PP chasing up SIC (width of hysteresis) satisfies

$$\begin{aligned} S &= \int_{T_{PCL_{2:1c}}}^{T_{PCL_{2:1c}}+H} (v_{PP} - v_{SIC}) dT_{PCL} \\ &= \int_{T_{PCL_{2:1c}}}^{T_{PCL_{2:1c}}+H} \left\{ 1 - \frac{f'[T_{DI}(2T_{PCL})]}{1 + f'[T_{DI}(2T_{PCL})]} \right\} dT_{PCL} \\ &= \int_{2T_{PCL_{2:1c}}}^{2T_{PCL_{2:1c}}+H} \frac{dT_{PCL}}{1 + f'[T_{DI}(2T_{PCL})]}. \end{aligned} \quad \text{(A1)}$$

Furthermore, there is another approach to calculate H without integrals: As we have already discussed in Sec. III, the location of SIC corresponds to the previous APD. Thus the location of each point on SIC can be given by

$$L_{SIC} = T_{APD} + R(I_{th}).$$

Note that $R(I_{th})$ may vary with I_{th}, but it remains to be a constant once I_{th} is set to be a benchmark equal to the pacing magnitude I_{st}, and can be determined from one measurement. At the critical point of transition from 1:1 to 2:1, PP locates at $PCL_{2:1c}$ and the steady APD is $T_{APD}(2T_{PCL_{2:1c}})$, so that SIC locates at

$$L_{SIC2:1c} = T_{APD}(2T_{PCL_{2:1c}}) + R(I_{th}).$$

The distance that PP has to walk to chase up SIC is the width of hysteresis H. H satisfies

$$T_{PCL_{2:1c}} + H = L_{SIC2:1c} + \Delta T_{APD},$$

where

$$\Delta T_{APD} = T_{APD}[2(T_{PCL_{2:1c}} + H)] - T_{APD}(2T_{PCL_{2:1c}})$$

Combining the above equations we obtain

$$T_{PCL_{2:1c}} + H = T_{APD}[2(T_{PCL_{2:1c}} + H)] + R(I_{th}). \quad \text{(A2)}$$

Both Eqs. (A1) and (A2) calculate H and they are essentially the same.

[1] G. R. Mines, J. Physiol. **46**, 349 (1913).
[2] S. Cukierman and P. de Carvalho A, J. Gen. Physiol. **79**, 1017 (1982).
[3] P. Lorente, C. Delgado, M. Delmar, D. Henzel, and J. Jalife, Circ. Res. **69**, 1301 (1991).
[4] M. Landau, P. Lorente, and S. C. J. Henry, J. Math. Biol. **25**, 491 (1987).
[5] M. L. Walker, X. Wan, G. E. Kirsch, and D. S. Rosenbaum, Circulation **108**, 2704 (2003).
[6] A. Vinet, J. Biol. Syst. **7**, 451 (1999).
[7] R. Wu and A. Patwardhan, Circ. Res. **94**, 634 (2004).
[8] G. M. Hall, S. Bahar, and D. J. Gauthier, Phys. Rev. Lett. **82**, 2995 (1999).
[9] A. R. Yehia, D. Jeandupeux, F. Alonso, and M. R. Guevara, Chaos **9**, 916 (1999).
[10] M. Delmar, J. Ibarra, J. Davidenko, P. Lorente, and J. Jalife, Circ. Res. **69**, 1316 (1991).
[11] D. R. Chialvo, D. C. Michaels, and J. Jalife, Circ. Res. **66**, 525 (1990).
[12] A. Vinet, D. R. Chialvo, D. C. Michaels, and J. Jalife, Circ. Res. **67**, 1510 (1990).
[13] V. Krinsky and A. Pumir, Chaos **8**, 188 (1998).
[14] S. W. Morgan, I. V. Biktasheva, and V. N. Biktashev, Phys. Rev. E **78**, 046207 (2008).
[15] A. Isomura, M. Hörning, K. Agladze, and K. Yoshikawa, Phys. Rev. E **78**, 066216 (2008).
[16] F. H. Fenton, E. M. Cherry, H. M. Hastings, and S. J. Evans, Chaos **12**, 852 (2002).
[17] V. N. Biktashev and A. V. Holden, Chaos **8**, 48 (1998).
[18] S. Sinha, A. Pande, and R. Pandit, Phys. Rev. Lett. **86**, 3678 (2001).
[19] M. Allessie, C. Kirchhof, G. J. Scheffer, F. Chorro, and J. Brugada, Circulation **84**, 1689 (1991).
[20] A. T. Stamp, G. V. Osipov, and J. J. Collins, Chaos **12**, 931 (2002).
[21] C. Luo and Y. Rudy, Circ. Res. **68**, 1501 (1991).
[22] S. Rush and H. Larsen, IEEE Trans. Biomed. Eng. **BME-25**, 389 (1978).
[23] D. R. Chialvo, R. F. Gilmour, and J. Jalife, Nature (London) **343**, 653 (1990).
[24] B. Nolasco and R. W. Dahlen, J. Appl. Physiol. **25**(2), 191 (1968).
[25] M. R. Guevara, G. Ward, A. Shier, and L. Glass, in Proceedings of the 11th Computers in Cardiology Conference (IEEE Computer Society, Los Angeles, 1984), p. 167.
[26] F. Xie, Z. Qu, A. Garfinkel, and J. N. Weiss, Am. J. Physiol. **283**, H448 (2002).
[27] J. F. Spear and E. N. Moore, Circ. Res. **35**, 782 (1974).
[28] T. J. Hund and Y. Rudy, Biophys. J. **79**, 3095 (2000).
[29] T. J. Lewis and M. R. Guevara, J. Theor. Biol. **146**, 407 (1990).
[30] B. Echebarria and A. Karma, Phys. Rev. Lett. **88**, 208101 (2002).
[31] M. Courtemanche, J. P. Keener, and L. Glass, SIAM J. Appl. Math. **56**, 119 (1996).
[32] P. Comtois and A. Vinet, Phys. Rev. E **68**, 051903 (2003).
[33] R. F. Gilmour, Jr., Drug Discovery Today **8**, 162 (2003).
[34] A. G. Kléber and Y. Rudy, Physiol. Rev. **84**, 431 (2004).
[35] G. W. Beeler and H. Reuter, J. Physiol. **268**, 177 (1977).
[36] J. J. Fox, J. L. McHarg, J. Robert F. Gilmour, Am. J. Physiol **282**, H516 (2002).
[37] M. Bär and M. Eiswirth, Phys. Rev. E **48**, R1635 (1993).
[38] R. Fitzhugh, Biophys. J. **1**, 445 (1961).
[39] A. T. Winfree, Chaos **1**, 303 (1991).
[40] A. T. Winfree, *When Time Breaks Down* (Princeton University Press, Princeton, NJ, 1987).
[41] Z. Cao, H. Zhang, F. Xie, and G. Hu, EPL **75**, 875 (2006).